

1 **Novel and unexpected genetic and microbial diversity for**
2 **arsenic cycling in deep sea cold seep sediments**

3 Chuwen Zhang¹, Xinyue Liu^{1,2}, Ling-Dong Shi³, Jiwei Li⁴,
4 Xi Xiao⁵, Zongze Shao^{1,6}, Xiyang Dong^{1,6*},

5 ¹ Key Laboratory of Marine Genetic Resources, Third Institute of Oceanography,
6 Ministry of Natural Resources, Xiamen, China

7 ² School of Marine Sciences, Sun Yat-Sen University, Zhuhai, China

8 ³ College of Environmental and Resource Sciences, Zhejiang University, Hangzhou,
9 China

10 ⁴ Institute of Deep-Sea Science and Engineering, Chinese Academy of Sciences,
11 Sanya, China

12 ⁵ Key Laboratory of Marine Mineral Resources, Ministry of Natural Resources,
13 Guangzhou Marine Geological Survey, China Geological Survey, Guangzhou, China

14 ⁶ Southern Marine Science and Engineering Guangdong Laboratory (Zhuhai), Zhuhai,
15 China

16

17 * Correspondence can be addressed to Xiyang Dong (dongxiyang@tio.org.cn).

18

19 **Abstract**

20 Cold seeps, where cold hydrocarbon-rich fluid escapes from the seafloor, showed
21 strong enrichment of toxic metalloid arsenic (As). The toxicity and mobility of As can
22 be greatly altered by microbial processes that play an important role in global As
23 biogeochemical cycling. However, a global overview of genes and microbes involved
24 in As transformation at seeps remains to be fully unveiled. Using 87 sediment
25 metagenomes and 33 metatranscriptomes derived from 13 globally distributed cold
26 seeps, we show that As resistance genes (*arsM*, *arsP*, *arsC1/arsC2*, *acr3*) were
27 prevalent at seeps and more phylogenetically diverse than previously expected.
28 Asgardarchaeota and a variety of unidentified bacterial phyla (e.g. 4484-113,
29 AABM5-125-24 and RBG-13-66-14) may also function as the key players in As
30 transformation. The abundances of As-cycling genes and the compositions of
31 As-associated microbiome shifted across different sediment depths or types of cold
32 seep. The energy-conserving arsenate reduction or arsenite oxidation could impact
33 biogeochemical cycling of carbon and nitrogen, via supporting carbon fixation,
34 hydrocarbon degradation and nitrogen fixation. Overall, this study provides a
35 comprehensive overview of As-cycling genes and microbes at As-enriched cold seeps,
36 laying a solid foundation for further studies of As cycling in deep sea microbiome at
37 the enzymatic and processual levels.

38 **Introduction**

39 Cold seeps are characterized by the emission of subsurface fluids into the sea floor
40 and occur widely at active and passive continental margins^{1,2}. The upward fluids are
41 often rich in methane and other hydrocarbons which sustain sea bed oases composed of
42 various microorganisms and faunal assemblages^{3,4}. The primary process that fuels
43 complex cold seep ecosystems is the anaerobic oxidation of methane (AOM),
44 conjointly operated by a consortium of anaerobic methane-oxidizing archaea (ANME)
45 and sulfate-reducing bacteria (SRB)^{5,6}. AOM removes approximately 80% of upward
46 venting methane, acting as an efficient methane filter⁷. Additionally, deep-sea cold seep
47 sediments also contain diverse and abundant diazotrophs that might contribute
48 substantially to the global nitrogen balance⁸. Cold seeps are therefore biologically and
49 geochemically significant on a global scale.

50 The venting fluids can significantly influence the sedimentary environment of seep
51 sites, resulting in changes of chemical characteristics of sediments⁹. In particular,
52 arsenic (As), one of the most abundant elements in the Earth's crust, are anomalously
53 enriched in seep sediments¹⁰⁻¹⁴. The anomalous As enrichment could be attributed to
54 the ascending fluids that could capture As and other metals when passing through
55 thick shaly formations^{10,14}; or the so-called particulate iron shuttle effect^{9,11,13}. As is
56 also a toxic metalloid in nature that, upon exposure, can cause negative effects for all
57 living things¹⁵. Depending on the physicochemical conditions, As can be found in
58 different oxidation and methylation states, showing various levels of toxicity and
59 bioavailability¹⁶. In marine environments, arsenate (As(V)), and arsenite (As(III)) are
60 the dominant forms of inorganic As¹⁷. It is assumed that microbes have evolved a
61 genetic repertoire related to As cycling, dated back to at least 2.72 billion years ago¹⁸,
62 ¹⁹. As biotransformation processes include As resistance (detoxification) to mitigate
63 toxicity and As respiration to conserve energy. The arsenic resistance is mainly
64 achieved by two steps: cytoplasmic reduction of As(V) to As(III) by the ArsC protein

65 and subsequent extrusion of As(III) via ArsB or Acr3 pump^{20, 21} (**Figure 1**). Another
66 As detoxification mechanism involves the methylation of As(III) to methylarsenite
67 (MAs(III)) by the ArsM enzyme²² (**Figure 1**). Although MAs(III) intermediates are
68 more toxic than As(III), they do not accumulate in cells and can be detoxified through
69 several different pathways. MAs(III) can be further methylated by ArsM and
70 volatilized, extruded from cells via the ArsP pump²³, oxidated to less toxic MAs(V)
71 by ArsH²⁴, or demethylated to less toxic As(III) by the ArsI lyase²⁵. As respiration
72 consists of the chemolithotrophic oxidation of As(III) by AioAB/ArxAB and
73 dissimilatory As(V) reduction by ArrAB^{15, 26} (**Figure 1**). Taken together, microbes
74 have a huge potential effect on the biogeochemical cycling and toxicity of As.

75 So far, As-transforming microbes and As-related genes have been widely investigated
76 in various natural environments, including polluted and pristine soils^{27, 28}, terrestrial
77 geothermal springs²⁹⁻³¹, wetlands^{32, 33}, pelagic oxygen-deficient zones³⁴,
78 groundwater³⁵, etc. For example, metagenomic and metatranscriptomic analyses
79 revealed that Aquificae are the key players for the *arsC*-based detoxification in
80 Tengchong geothermal springs²⁹. A global survey also described the phylogenetic
81 diversity, genomic location, and biogeography of As-related genes in soil
82 metagenomes³⁶. Only recently, the behavior of As biotransformation has been
83 reported in the deep-sea realms, i.e. hadal trench of the Challenger Deep³⁷. Deep-sea
84 ecosystems cover 67% of Earth surface and have extremely high densities of microbes
85 (up to 1000× greater than surface waters) which play a critical role for long-term
86 controls on global biogeochemical cycles^{38, 39}. The environmental conditions in deep
87 seafloor cold seeps differ greatly from those in the aforementioned ecosystems, such
88 as low temperatures, high pressure, darkness and the presence of seepage activities¹.
89 Thus, the investigation of As-related genes and microbes at seeps will expand our
90 current knowledge on As metabolisms and allow us to discover new lineages
91 containing As-related genes.

92 The purpose of this study was to decipher the microbial transformation of As in cold
93 seep sediments at a global scale. Here, we applied a relatively comprehensive data set
94 of 87 sediment metagenomes and 33 metatranscriptomes derived from 13
95 geographically diverse cold seeps across global oceans (**Table S1**), to investigate
96 As-associated genes and their host microbes. This study aims to address the following
97 questions: (i) biogeography of As-cycling genes across global cold seeps; (ii)
98 phylogenetic diversity and distribution of As-cycling genes across global cold seeps;
99 (iii) interactions between As metabolisms and biogeochemical cycles of carbon and
100 nitrogen.

101 **Results and discussion**

102 **As cycling genes are widespread and active across global cold seeps**

103 To gain a broad view on biogeography of As cycling genes, we determined their
104 abundance from 87 sediment metagenomes collected from 13 globally distributed cold
105 seeps. For comparison, we also calculated the abundance of *dsrA* genes whose products
106 catalyzing the well-studied and predominated metabolic processes in cold seep
107 ecosystems, i.e. sulfur oxidation and reduction⁴⁰. We found that genes related to As
108 resistance are prevalent in these cold seep samples (**Figure 2**) and their abundances are
109 higher than those of *dsrA* genes (**Figure S2-S3; Table S2**). The *arsM* and *arsP* genes
110 that respectively produce volatilized methylated organoarsenicals and mediate its
111 subsequent expulsion outside cell, were the most abundant ones. The *arsC1/arsC2*
112 genes for cytoplasmic As(V) reduction and the *acr3* gene for As(III) extrusion also
113 dominated most cold seep samples. Moreover, As resistance genes, i.e. *arsM*, *arsP*,
114 *arsC1/arsC2*, *acr3*, were actively expressed in the sediment metatranscriptomes from
115 Haima and Jiaolong seeps along with gas hydrate deposit zones of Qiongdongnan and
116 Shenhu, revealing *in situ* microbial activities on As detoxification (**Figure S4**). Seep
117 microbes might utilize both methylation and cytoplasmic As(V) reduction strategies to

118 overcome potential toxic effects of exceptional As accumulation at cold seeps.
119 Alternatively, methylation is not strictly a detoxification pathway but also an
120 antibiotic-producing process with MAs(III) being a primitive antibiotic⁴¹, which could
121 provide additional survival advantages. However, the function of *ArsM* in anoxic
122 environments and its contribution to As cycling have yet to be verified. Our results
123 contradict previous findings demonstrating that *arsM* are less common in soils³⁶ and
124 hot springs²⁹ than *arsC*, but in line with those found in hadal sediments³⁷. The
125 discrepancy in As detoxification mechanisms between terrestrial and deep-sea
126 ecosystems could be attributed to their huge variations in the habitats and geographical
127 locations. When comparing the abundance of As(III) efflux pumps, we observed that
128 *arsB* was in much lower abundance than *acr3* (**Figure 2a**). Previous studies also
129 reported an abundance of *acr3* over *arsB* in forest soils and wetlands^{32, 36, 42}. This is
130 likely because *Acr3* proteins are more ancient and have greater phylogenetic
131 distribution as compared with *ArsB*¹⁹. Conversely, genes related to energetic arsenic
132 respiratory oxidation (*aioA*) and reduction (*arrA/arsA*) were less abundant in all cold
133 seep samples as compared with arsenic detoxification genes. Despite of this, respiratory
134 genes were transcriptionally active, as evidenced by the detection of *arrA* transcripts in
135 Jiaolong seep (up to 15.9 TPM, **Figure S4**).

136 To determine the distribution characteristics of As cycling genes, each metagenome
137 was categorized in terms of its sediment depth (i.e. surface: <1 mbsf; shallow: 1-10
138 mbsf; deep: >10 mbsf). Metagenomes were also grouped based on the type of cold seep,
139 including gas hydrate, seep (i.e. oil and gas/methane seep), and volcano (mud/asphalt
140 volcano)¹, respectively. The partial least squares discrimination analysis (PLS-DA)
141 revealed dissimilarity in As cycling genes among different sediment layers (**Figure 2b**;
142 $F = 4.3504$, $p = 0.001$, $R^2 = 0.10267$, 999-permutations PERMANOVA test). The
143 distribution traits of As cycling genes in surface sediments were separated from deep
144 sediments and more similar to those in shallow ones (**Figure 2b**). The abundance of
145 prevalent As cycling genes such as *acr3*, *arsC2* and *arsM* in deep sediments were

146 significantly higher as compared with those in shallow and surface sediments (**Figure**
147 **S2**). As cycling genes in different types of cold seep were also different from each other
148 (**Figure 2b**; $F = 3.5246$, $p = 0.004$, $R^2 = 0.07742$, 999-permutations PERMANOVA
149 test). Dominant As cycling genes in gas hydrates displayed higher abundances as
150 compared with those in seeps and volcanos (**Figure S3**). Hence, the distributions of
151 As-associated genes were influenced by a combination of sediment depths and types of
152 cold seep. The higher As-cycling gene abundance observed in our deep or gas
153 hydrate-associated samples could be correlated with a high level of environmental As,
154 as what described in As-rich altiplanic wetland³². In the Nankai Trough, As with
155 unknown sources was demonstrated to actively release into sediments layers where
156 methane hydrates occur (As concentration of 14 ppm in gas hydrate-bearing sediments
157 vs av. 6.4 ppm for the whole sediment core)¹⁷.

158 **Microbes involved in As cycling varied between seep habitats**

159 To profile taxonomic diversity of As-related microbes, a total of 1741 species-level
160 metagenome-assembled genomes (MAGs, 95% average nucleotide identity) were
161 reconstructed from these 87 cold seep metagenomes (**Table S3**). Of these, 1083 MAGs
162 spanning 9 archaeal and 63 bacterial phyla as well as one unclassified bacterial phylum
163 were potentially involved in As cycling at cold seeps (**Table S4**). Metagenomic read
164 recruitments revealed that the recovered 1083 arsenic-related MAGs accounted for
165 1.8-62.8% cold seep communities (**Figure 3 and Table S4**). Taxonomic compositions
166 of As-related microbiomes across different types of cold seep displayed pronounced
167 variations (**Figure 3**). In the sediments derived from oil and gas/methane seep,
168 arsenic-related microbes contained mostly Methanogasteraceae (i.e. ANME-2c) and
169 Methanocomedenaceae (i.e. ANME-2a) within Halobacteriota phylum, ETH-SRB1
170 within Desulfobacterota phylum, JS1 within Atribacterota phylum as well as
171 Anaerolineae and Dehalococcoidia within Chloroflexota phylum. The As-related
172 microbes in gas hydrate sediments were dominated by bacterial lineages, highlighted

173 by Atribacterota (JS1) and Chloroflexota (Anaerolineae and Dehalococcoidia).
174 Nevertheless, in asphalt/mud volcano sediments, the compositions of arsenic-related
175 microbes were diverse in different samples. The clear distinctions in As-related
176 microbiomes between different seep habitats suggested an important role driven by
177 environment selection. Multiple parameters, including sediment temperature, sediment
178 depth, water depth, methane concentration, and geographic distance have been
179 demonstrated to cause these variations^{43, 44}.

180 **Expanded diversity of microbial lineages containing As resistance genes**

181 Among these As resistance genes, *acr3*, *arsC1/arsC2*, *arsM* and *arsP* were widely
182 distributed in bacteria and archaea, while other As resistance genes (*arsB*, *arsI* and
183 *arsH*) were sparsely distributed (**Figure 4**). The *acr3* gene is typically affiliated with
184 Proteobacterial, Firmicutes Actinobacterial and other bacterial sequences^{36, 42, 45}. Our
185 study observed an unexpectedly wider phylogenetical diversity of *acr3* than previously
186 reported. Notably, Asgardarchaeota including Lokiarchaeia, Thorarchaeia, Sifarchaeia,
187 LC30, along with Heimdallarchaeia and Wukongarchaeia described as the most likely
188 sister group of eukaryotes, are firstly documented to have genetically capability for
189 As(III) extrusion. The greater diversity of As resistance genes found in
190 Asgardarchaeota phylum further point to their ancient origin¹⁹. Furthermore, a
191 considerable number of candidate bacterial phyla without cultured representatives (e.g.
192 4484-113, AABM5-125-24 and RBG-13-66-14) were also equipped with such an
193 ability. Though their functional redundancy as As(III) efflux pumps, *arsB* was more
194 phylogenetically conserved as compared with *acr3* and simply restricted to
195 Alphaproteobacteria, Gammaproteobacteria and Campylobacterota (**Figure 4**). This
196 observation is in agreement with previous reports comparing the diversity of *arsB* to
197 *acr3*^{36, 42, 45}. The *arsM* gene was relatively uncommon in terrestrial soil
198 microorganisms^{29, 36}. In contrast, this study showed that the *arsM* genes in seep
199 microbes have a great taxonomic diversity similar to *acr3* gene, including

200 Chloroflexota, Proteobacteria, Atribacterota, Asgardarchaeota, Hydrothermarchaeota,
201 Thermoplasmata, Thermoproteota as well as other currently unidentified bacterial
202 phyla (e.g. 4484-113, AABM5-125-24 and RBG-13-66-14) (**Figure 4**). Among these,
203 Atribacterota, Asgardarchaeota and the candidate bacterial phyla stated above have not
204 previously been implicated in As methylation^{19, 36}. For cytoplasmic As(V) reduction,
205 Asgard archaeal lineages all lacked corresponding genes (*arsC1* and *arsC2*). In general,
206 these data advance our understanding on the phylogenetical diversity of As resistance
207 genes and highlight the potentially important role played by archaea in As cycling,
208 Asgardarchaeota particularly.

209 **Novel seep lineages are identified to perform As respiration**

210 In addition to mitigating toxicity, some microorganisms can respire the redox-sensitive
211 element of As to reap energetic gains (i.e. arsenotrophy), either via chemoautotrophic
212 As(III) oxidation (*aioAB/arxAB*) or anaerobic As(V) respiration (*arrAB*)^{46, 47}. The
213 alpha subunits of these arsenotrophic enzymes form distinct clades with the
214 dimethylsulfoxide (DMSO) reductase superfamily³⁴. This superfamily also includes
215 other enzymes critical in respiratory redox transformations, e.g. Nap and Nar. Here,
216 we identified two AioA, three ArxA and 17 ArrA protein sequences, respectively. A
217 phylogenetic analysis of recovered arsenotrophic protein sequences showed that they
218 all clustered together with known AioA/ArxA and ArrA proteins (**Figure 5a**).
219 Functional As bioenergetic *aioA/arxA* and *arrA* genes are generally found together
220 with other necessary accessory genes. The *aioA* of As(III) oxidizing microorganisms
221 always forms an operon with *aioB* and other genes involved in As resistance and
222 metabolisms (e.g. *aioD*, *aioXSR*, *arsR*)^{15, 26}. Arx is demonstrated to be a variant of Arr
223 and these two enzymes have a similar genetic arrangement. The *arrA/arxA* gene is
224 always found together with the *arrB/arxB* and often with the *arrC/arxC* and
225 *arrD/arxD*^{15, 26}. The genomic organization analysis showed that identified two *aioA*,
226 three *arxA* and 11 of 17 *arrA* genes all have corresponding accessory genes (**Figure**

227 **5b)**, further confirming their potential identities as arsenotrophic enzymes.

228 The *aioA/arrA* genes are uncommon in soil microbiomes and mostly found in
229 Proteobacteria^{15, 36, 48}. By assigning the taxonomy, *aioA/arrA* genes recovered here
230 belong to Gammaproteobacteria (n=3) and Alphaproteobacteria (n=2), consistent with
231 previous findings (**Figure 3 and Figure 5c**). Nevertheless, 17 *arrA* genes were
232 phylogenetically affiliated with seven distinct bacterial lineages: Bacteroidota (n=1),
233 Chloroflexota (n=4), Deferribacterota (n=1), Desulfobacterota (n=8),
234 Desulfobacterota_I (n=1), Gammaproteobacteria (n=1), and Nitrospirota (n=1) (**Figure**
235 **3 and Figure 5c**). Despite that several other bacterial lineages (i.e. Deferribacterota,
236 Firmicutes and Chrysiogenetes) are reported to contain *arrA* genes, most known
237 As(V)-respiring microorganisms are assigned to proteobacterial clades^{15, 36, 48}. Our
238 findings, the *arrA*-containing Bacteroidota, Chloroflexota and Nitrospirota, expand the
239 database of putative dissimilatory As(V) reducers.

240 **As respiration are potentially critical to central metabolisms in cold seeps**

241 Microbially mediated As respiration has been verified to influence biogeochemical
242 cycles of carbon and nitrogen, e.g. chemoautotrophic As(III) oxidation coupled with
243 denitrification^{49, 50}. Here, functional annotation identified near-complete calvin and
244 reductive TCA carbon fixation pathways in *aioA/arrA*-carrying Alphaproteobacteria
245 (n=2) and Gammaproteobacteria MAGs (n=3) (**Figure 5c**). Terminal reductase
246 systems were also recognized in *aioA/arrA*-carrying MAGs, i.e. nitrate reductase
247 (*narGHI*). The cooccurrence of these genes suggests that the As(III) oxidation may
248 help support autotrophic carbon fixation and nitrate reduction.

249 In addition, five *arrA*-carrying MAGs possessed genes for AssA (**Figure 5c**), which
250 mediate the first step of anaerobic activation of alkanes via fumarate addition.
251 Phylogenetic analyses revealed that identified AssA sequences were phylogenetically
252 close to archaea-type and Group V AssA⁵¹ (**Figure S5**). These potential hydrocarbon

253 degraders were classified as Chloroflexota (n=2), Deferribacterota (n=1),
254 Desulfobacterota (n=1), and Bacteroidota (n=1). Methane, the simplest hydrocarbon,
255 has been demonstrated to stimulate As(V) respiration during the process of anaerobic
256 oxidation of methane⁵². Similarly, the occurrence of both *AssA* and *ArrA* indicated that
257 heterotrophic MAGs stated above may also employ As(V) as electron acceptor for
258 anaerobic degradation of multi-carbon alkanes. Genes encoding carbohydrate-active
259 enzymes (CAZymes) targeting various complex carbohydrates were also present in
260 these arsenotrophic MAGs, including chitin, pectin, starch and polyphenolics (**Figure**
261 **5c**).

262 Notably, arsenotrophic MAGs may function as potential nitrogen fixers introducing
263 new N to local environment. Genes encoding for the catalytic component of
264 nitrogenase (i.e. *nifHDK*) were detected in one *arxA*-carrying (Gammaproteobacteria,
265 n=1) and six *arrA*-carrying (Gammaproteobacteria, n=1; Desulfobacterota, n=4;
266 Desulfobacterota_I, n=1) MAGs (**Figure 5c**). It has been previously reported that
267 As(III) oxidation can fuel biological nitrogen fixation in tailing and
268 metal(loid)-contaminated soils^{53, 54}. The data present here further complement that
269 diazotrophs could also fix N₂ using energy obtained from dissimilatory As(V)
270 reduction.

271 Our findings point towards a previously unrecognized arsenotrophs at seeps,
272 impacting both carbon and nitrogen cycling. However, we acknowledge that
273 cultivation experiments with As-respiring isolates are ultimately needed both to
274 elucidate their lifestyle and confirm functionality for As-dependent carbon fixation,
275 hydrocarbon and carbohydrate degradation as well as nitrogen fixation.

276 **Conclusions**

277 Microbial transformation of As has been well documented and characterized in
278 environments in such as ocean water, groundwater and geothermal springs, but the

279 knowledge on gene- and genome-level As cycling in deep sea (e.g. cold seep) is limited.
280 Our study demonstrated that As methylation and cytoplasmic As(V) reduction were the
281 predominant detoxification mechanisms employed by cold seep microbiomes. These
282 results substantially expanded the diversity of As resistance genes to a broader
283 microbial community including Asgardarchaeota and a great number of candidate
284 bacterial phyla. In addition, novel arsenotrophic lineages are also identified, including
285 Bacteroidota, Chloroflexota, Nitrospirota, etc, which also potentially participate in
286 carbon and nitrogen biogeochemical cycling. This study provides a detailed
287 understanding of As biotransformation in a complex microbiome in deep-sea realms,
288 which could have significant implications for addressing environmental issues. The
289 identification of arsenotrophic microbes will also enable proxies for arsenic-based
290 metabolisms in early anoxic oceans.

291 **Methods**

292 **Metagenomic and metatranscriptomic data sets**

293 The 87 metagenomes and 33 metatranscriptomes analyzed in this study are derived
294 from 13 globally distributed cold seep sites (**Figure S1**). Among them, 65
295 metagenomes and 10 metatranscriptomes were compiled from our previous
296 publications^{8,55}, and other 22 metagenomes were downloaded from NCBI Sequencing
297 Read Archive (SRA). A detailed description of sampling locations and sequencing
298 information for metagenomic and metatranscriptomic data is given in **Table S1**.

299 **Bioinformatic analyses**

300 DNA reads pre-processing, metagenomic assembly and binning were performed with
301 the function modules of metaWRAP (v1.3.2)⁵⁶. First, the metaWRAP Read_qc module
302 was used to trim raw sequencing DNA reads. Then the filtered DNA reads were

303 individually assembled with the metaWRAP Assembly module using Megahit⁵⁷ or
304 metaSPAdes⁵⁸ with default settings (detailed assembly statistics are summarized in
305 Table S1). In addition, metagenomic reads from the same sampling station (n=10) were
306 also co-assembled using Megahit with the default settings. Thereafter, MAGs were
307 recovered from contigs with the length longer than 1kb using the metaWRAP Binning
308 module (parameters: -maxbin2 -concoct -metabat2) or the VAMB tool⁵⁹ (v3.0.1;
309 default parameters; detailed binning statistics are summarized in **Table S1**). Further
310 refinement of MAGs was performed by the Bin_refinement module of metaWRAP
311 (parameters: -c 50 -x 10), and CheckM (v1.0.12)⁶⁰ was used to estimate the
312 completeness and contamination of these MAGs. All MAGs were dereplicated at 95%
313 average nucleotide identity (ANI) using dRep (v3.4.0; parameters: -comp 50 -con 10)⁶¹
314 to obtain representative species MAGs. This analysis provided a non-redundant
315 genome set consisting of 1,741 species-level MAGs.

316 Raw metatranscriptomes were quality filtered with the Read_qc module of metaWRAP
317 (v1.3.2)⁵⁶ as described above. The removal of ribosomal RNAs was conducted with
318 sortmeRNA (v2.1)⁶² in the quality-controlled metatranscriptomic reads.

319 **Non-redundant gene catalog construction**

320 Genes were predicted on contigs (≥ 1 kb) from the assemblies using the METABOLIC
321 pipeline (v4.0)⁶³, which resulted in 33,799,667 protein-coding genes. Clustering of the
322 predicted proteins was performed with MMseqs2 (v13.45111)⁶⁴ using the cascaded
323 clustering algorithm at 95% sequence similarity and 90% sequence coverage
324 (parameters: -c 0.95 -min-seq-id 0.95 -cov-mode 1 -cluster-mode 2) following the ref.⁶⁵.
325 This process yielded a total of 17,217,131 non-redundant gene clusters.

326 **Searching for arsenic cycling genes**

327 In this study, 11 well-characterized marker genes^{66, 67} were selected to assess their

328 potential influence to the arsenic biogeochemical cycle. These genes include eight
329 arsenic resistance genes (*acr3*, *arsB*, *arsC1*, *arsC2*, *arsP*, *arsH*, *arsI*, and *arsM*) and
330 three arsenic respiratory genes (*aioA*, *arrA*, and *arxA*). A hidden Markov model
331 (HMM)-based search was performed to identify arsenic-related genes in
332 non-redundant gene catalogue by using *hmmsearch* function in HMMER package
333 (v3.1b2)⁶⁸. The HMM profile searches and score cutoffs for 11 arsenic-related genes
334 were taken from Lavy et al. (2020)⁶⁷.

335 **Taxonomic and functional profiling of MAGs**

336 Arsenic-related MAGs were taxonomically annotated using the *classify_wf* function of
337 the GTDB-Tk toolkit (v2.1.1)⁶⁹ with default parameters against the GTDB r207 release.
338 For all MAGs, gene calling and metabolic pathway prediction were conducted with
339 the METABOLIC pipeline (v4.0)⁶³. Functional annotation of genomes was also carried
340 out by searching against KEGG, Pfam, MEROPS and dbCAN databases using DRAM
341 (v1.3.5)⁷⁰. The identification of arsenic-related genes in MAGs was performed by
342 searching against As-related HMM profiles from Lavy et al. (2020)⁶⁷ as reported above.
343 Genes involved in anaerobic hydrocarbon degradation were screened using BLASTp
344 (identity >30%, coverage >90%, $e < 1 \times 10^{-20}$) against local protein databases⁵¹.

345 **Abundance calculations**

346 For contig level, the relative abundance of genes related to arsenic cycling across 87
347 metagenomes were calculated from non-redundant gene catalog using the program
348 Salmon (v1.9.0)⁷¹ in the mapping-based mode (parameters: *-validateMappings -meta*).
349 GPM (genes per million) values were used as a proxy for gene abundance as describe
350 in ref.⁷⁰. For genome level, the relative abundance of each MAG was profiled by
351 mapping quality-trimmed reads from the 87 metagenomes against the MAGs using
352 CoverM in genome mode (<https://github.com/wwood/CoverM>) (v0.6.1; parameters:

353 -min-read-percent-identity 0.95 -min-read-aligned-percent 0.75 -trim-min 0.10
354 -trim-max 0.90 -m relative_abundance).

355 To calculate the transcript abundance of As-related genes, we also mapped clean reads
356 from the 33 metatranscriptomes to non-redundant gene catalog. The transcript
357 abundance of each gene was calculated as the metric-TPM (transcripts per million).

358 **Phylogenetic analyses of functional genes**

359 For phylogeny inference, protein sequences of functional genes were aligned with
360 MAFFT (v7.490, -auto option)⁷², and gap sequences were trimmed using trimAl (v.
361 1.2.59, -automated1 option)⁷³. Maximum likelihood phylogenetic trees were
362 constructed for each genes using IQ-TREE (v2.12)⁷⁴ with the following options: -m
363 TEST -bb 1000 -alrt 1000. Branch support was estimated using 1000 replicates of both
364 ultrafast bootstrap approximation (UFBoot)) and Shimodaira-Hasegawa (SH)-like
365 approximation likelihood ratio (aLRT). Reference protein sequences for As-based
366 respiratory cycle were obtained from Saunders et al. (2019)³⁴. Reference protein
367 sequences for fumarate addition were derived from Zhang et al. (2021)⁵¹. All the tree
368 files were uploaded to Interactive tree of life (iTOL; v6)⁷⁵ for visualization and
369 annotation.

370 **Statistical analyses**

371 Statistical analyses were done in R (v4.0.4-v4.1.0) with the following descriptions.
372 Normality and homoscedasticity of data were evaluated using Shapiro-Wilk test and
373 Levene's test, respectively. One-way analysis of variance (ANOVA) and least
374 significant difference (LSD) test were conducted to evaluate the variations of each gene
375 across different sediment depths and types of cold seeps. The partial least squares
376 discrimination analysis (PLS-DA) was performed based on the GPM values of
377 arsenic-cycling genes with R package 'mixOmics'. The permutational multivariate

378 analysis of variance (PERMANOVA) was employed to test whether arsenic-cycling
379 genes shifted among different sediment depths and types of cold seeps using ‘adonis’
380 function in vegan package. All PERMANOVA tests were performed with 9999
381 permutations based on Bray–Curtis dissimilarity.

382 **DATA AVAILABILITY**

383 Genes and MAGs with As cycling genes, and files for the phylogenetic trees were
384 deposited in Figshare (<https://doi.org/10.6084/m9.figshare.21550431>).

385

386 **References**

- 387 1. Joye, S. B., The Geology and Biogeochemistry of Hydrocarbon Seeps. *Annual Review of Earth*
388 *and Planetary Sciences* **2020**, 48(1), 205-231.
- 389 2. Feng, D.; Qiu, J.-W.; Hu, Y.; Peckmann, J.; Guan, H.; Tong, H.; Chen, C.; Chen, J.; Gong, S.; Li,
390 N.; Chen, D., Cold seep systems in the South China Sea: An overview. *Journal of Asian Earth Sciences*
391 **2018**, 168(3-16).
- 392 3. Dubilier, N.; Bergin, C.; Lott, C., Symbiotic diversity in marine animals: the art of harnessing
393 chemosynthesis. *Nature Reviews Microbiology* **2008**, 6(10), 725-740.
- 394 4. Levin, L. A., ECOLOGY OF COLD SEEP SEDIMENTS: INTERACTIONS OF FAUNA WITH
395 FLOW, CHEMISTRY AND MICROBES. *Oceanography and Marine Biology* **2005**, 43(11-56).
- 396 5. Dong, X.; Rattray, J. E.; Campbell, D. C.; Webb, J.; Chakraborty, A.; Adebayo, O.; Matthews, S.;
397 Li, C.; Fowler, M.; Morrison, N. M.; MacDonald, A.; Groves, R. A.; Lewis, I. A.; Wang, S. H.; Mayumi,
398 D.; Greening, C.; Hubert, C. R. J., Thermogenic hydrocarbon biodegradation by diverse depth-stratified
399 microbial populations at a Scotian Basin cold seep. *Nature communications* **2020**, 11(1), 5825-5825.
- 400 6. Kleindienst, S.; Herbst, F.-A.; Stagars, M.; von Netzer, F.; von Bergen, M.; Seifert, J.; Peplies, J.;
401 Amann, R.; Musat, F.; Lueders, T.; Knittel, K., Diverse sulfate-reducing bacteria of the
402 *Desulfosarcina/Desulfococcus* clade are the key alkane degraders at marine seeps. *The ISME Journal*
403 **2014**, 8(10), 2029-2044.
- 404 7. Reeburgh, W. S., Oceanic methane biogeochemistry. *Chemical reviews* **2007**, 107(2), 486-513.
- 405 8. Dong, X.; Zhang, C.; Peng, Y.; Zhang, H.-X.; Shi, L.-D.; Wei, G.; Hubert, C. R. J.; Wang, Y.;
406 Greening, C., Phylogenetically and catabolically diverse diazotrophs reside in deep-sea cold seep
407 sediments. *Nature Communications* **2022**, 13(1), 4885.
- 408 9. Wang, Q.; Chen, D.; Peckmann, J., Iron shuttle controls on molybdenum, arsenic, and antimony
409 enrichment in Pliocene methane-seep carbonates from the southern Western Foothills, Southwestern
410 Taiwan. *Marine and Petroleum Geology* **2019**, 100(263-269).
- 411 10. Tribovillard, N.; du Châtelet, E. A.; Gay, A.; Barbécot, F.; Sansjofre, P.; Potdevin, J.-L.,
412 Geochemistry of cold seepage-impacted sediments: Per-ascensum or per-descensum trace metal
413 enrichment? *Chemical Geology* **2013**, 340(1-12).

- 414 11. Hu, Y.; Feng, D.; Peckmann, J.; Roberts, H. H.; Chen, D., New insights into cerium anomalies and
415 mechanisms of trace metal enrichment in authigenic carbonate from hydrocarbon seeps. *Chemical*
416 *Geology* **2014**, 381(55-66).
- 417 12. Carvalho, L.; Monteiro, R.; Figueira, P.; Mieiro, C.; Almeida, J.; Pereira, E.; Magalhães, V.;
418 Pinheiro, L.; Vale, C., Vertical distribution of major, minor and trace elements in sediments from mud
419 volcanoes of the Gulf of Cadiz: evidence of Cd, As and Ba fronts in upper layers. *Deep Sea Research*
420 *Part I: Oceanographic Research Papers* **2018**, 131(133-143).
- 421 13. Tribovillard, N., Arsenic in marine sediments: how robust a redox proxy? *Palaeogeography,*
422 *Palaeoclimatology, Palaeoecology* **2020**, 550(109745).
- 423 14. Cangemi, M.; Di Leonardo, R.; Bellanca, A.; Cundy, A.; Neri, R.; Angelone, M., Geochemistry
424 and mineralogy of sediments and authigenic carbonates from the Malta Plateau, Strait of Sicily (Central
425 Mediterranean): Relationships with mud/fluid release from a mud volcano system. *Chemical Geology*
426 **2010**, 276(3), 294-308.
- 427 15. Andres, J.; Bertin, P. N., The microbial genomics of arsenic. *FEMS Microbiology Reviews* **2016**,
428 40(2), 299-322.
- 429 16. Rahman, M. A.; Hassler, C., Is arsenic biotransformation a detoxification mechanism for
430 microorganisms? *Aquatic Toxicology* **2014**, 146(212-219).
- 431 17. Masuda, H.; Yoshinishi, H.; Fuchida, S.; Toki, T.; Even, E., Vertical profiles of arsenic and arsenic
432 species transformations in deep-sea sediment, Nankai Trough, offshore Japan. *Progress in Earth and*
433 *Planetary Science* **2019**, 6(1), 28.
- 434 18. Sforza, M. C.; Philippot, P.; Somogyi, A.; van Zuilen, M. A.; Medjoubi, K.; Schoepp-Cothenet, B.;
435 Nitschke, W.; Visscher, P. T., Evidence for arsenic metabolism and cycling by microorganisms 2.7
436 billion years ago. *Nature Geoscience* **2014**, 7(11), 811-815.
- 437 19. Chen, S.-C.; Sun, G.-X.; Yan, Y.; Konstantinidis, K. T.; Zhang, S.-Y.; Deng, Y.; Li, X.-M.; Cui,
438 H.-L.; Musat, F.; Popp, D.; Rosen, B. P.; Zhu, Y.-G., The Great Oxidation Event expanded the genetic
439 repertoire of arsenic metabolism and cycling. *Proceedings of the National Academy of Sciences* **2020**,
440 117(19), 10414.
- 441 20. Rosen, B. P., Biochemistry of arsenic detoxification. *FEBS Letters* **2002**, 529(1), 86-92.
- 442 21. Mukhopadhyay, R.; Rosen, B. P., Arsenate reductases in prokaryotes and eukaryotes.
443 *Environmental health perspectives* **2002**, 110 Suppl 5(Suppl 5), 745-8.
- 444 22. Qin, J.; Rosen, B. P.; Zhang, Y.; Wang, G.; Franke, S.; Rensing, C., Arsenic detoxification and
445 evolution of trimethylarsine gas by a microbial arsenite S-adenosylmethionine methyltransferase.
446 *Proceedings of the National Academy of Sciences* **2006**, 103(7), 2075-2080.
- 447 23. Chen, J.; Madegowda, M.; Bhattacharjee, H.; Rosen, B. P., ArsP: a methylarsenite efflux
448 permease. *Molecular Microbiology* **2015**, 98(4), 625-635.
- 449 24. Chen, J.; Bhattacharjee, H.; Rosen, B. P., ArsH is an organoarsenical oxidase that confers
450 resistance to trivalent forms of the herbicide monosodium methylarsenate and the poultry growth
451 promoter roxarsone. *Molecular Microbiology* **2015**, 96(5), 1042-1052.
- 452 25. Yoshinaga, M.; Rosen, B. P., A C·As lyase for degradation of environmental organoarsenical
453 herbicides and animal husbandry growth promoters. *Proceedings of the National Academy of Sciences*
454 **2014**, 111(21), 7701-7706.
- 455 26. Rascovan, N.; Maldonado, J.; Vazquez, M. P.; Eugenia Fariás, M., Metagenomic study of red

- 456 biofilms from Diamante Lake reveals ancient arsenic bioenergetics in haloarchaea. *The ISME Journal*
457 **2016**, 10(2), 299-309.
- 458 27. Zhang, S. Y.; Xiao, X.; Chen, S. C.; Zhu, Y. G.; Sun, G. X.; Konstantinidis, K. T., High Arsenic
459 Levels Increase Activity Rather than Diversity or Abundance of Arsenic Metabolism Genes in Paddy
460 Soils. *Appl Environ Microbiol* **2021**, 87(20), e0138321.
- 461 28. Shi, L.-D.; Zhou, Y.-J.; Tang, X.-J.; Kappler, A.; Chistoserdova, L.; Zhu, L.-Z.; Zhao, H.-P.,
462 Coupled Aerobic Methane Oxidation and Arsenate Reduction Contributes to Soil-Arsenic Mobilization
463 in Agricultural Fields. *Environmental Science & Technology* **2022**.
- 464 29. Yin, Z.; Ye, L.; Jing, C., Genome-Resolved Metagenomics and Metatranscriptomics Reveal that
465 Aquificae Dominates Arsenate Reduction in Tengchong Geothermal Springs. *Environmental Science &*
466 *Technology* **2022**.
- 467 30. Hug, K.; Maher, W. A.; Stott, M. B.; Krikowa, F.; Foster, S.; Moreau, J. W., Microbial
468 contributions to coupled arsenic and sulfur cycling in the acid-sulfide hot spring Champagne Pool, New
469 Zealand. *Frontiers in Microbiology* **2014**, 5(
- 470 31. Zhang, S.-Y.; Zhao, F.-j.; Sun, G.; Su, J.; Yang, X.-R.; Li, H.; Zhu, Y.-g., Diversity and abundance
471 of arsenic biotransformation genes in paddy soils from southern China. *Environmental science &*
472 *technology* **2015**, 49 7(4138-46.
- 473 32. Castro-Severyn, J.; Pardo-Esté, C.; Mendez Katterinne, N.; Fortt, J.; Marquez, S.; Molina, F.;
474 Castro-Nallar, E.; Remonsellez, F.; Saavedra Claudia, P., Living to the High Extreme: Unraveling the
475 Composition, Structure, and Functional Insights of Bacterial Communities Thriving in the
476 Arsenic-Rich Salar de Huasco Altiplanic Ecosystem. *Microbiology Spectrum* **2021**, 9(1), e00444-21.
- 477 33. Zhang, S.-Y.; Su, J.-Q.; Sun, G.-X.; Yang, Y.; Zhao, Y.; Ding, J.; Chen, Y.-S.; Shen, Y.; Zhu, G.;
478 Rensing, C.; Zhu, Y.-G., Land scale biogeography of arsenic biotransformation genes in estuarine
479 wetland. *Environmental Microbiology* **2017**, 19(6), 2468-2482.
- 480 34. Saunders, J. K.; Fuchsman, C. A.; McKay, C.; Rocap, G., Complete arsenic-based respiratory
481 cycle in the marine microbial communities of pelagic oxygen-deficient zones. *Proceedings of the*
482 *National Academy of Sciences* **2019**, 116(20), 9925.
- 483 35. Wang, L.; Yin, Z.; Jing, C., Metagenomic insights into microbial arsenic metabolism in shallow
484 groundwater of Datong basin, China. *Chemosphere* **2020**, 245(125603.
- 485 36. Dunivin, T. K.; Yeh, S. Y.; Shade, A., A global survey of arsenic-related genes in soil microbiomes.
486 *BMC Biology* **2019**, 17(1), 45.
- 487 37. Zhou, Y.-L.; Mara, P.; Cui, G.-J.; Edgcomb, V. P.; Wang, Y., Microbiomes in the Challenger Deep
488 slope and bottom-axis sediments. *Nature Communications* **2022**, 13(1), 1515.
- 489 38. Jørgensen, B. B.; Boetius, A., Feast and famine — microbial life in the deep-sea bed. *Nature*
490 *Reviews Microbiology* **2007**, 5(10), 770-781.
- 491 39. Orcutt, B. N.; Sylvan, J. B.; Knab, N. J.; Edwards, K. J., Microbial ecology of the dark ocean
492 above, at, and below the seafloor. *Microbiol Mol Biol Rev* **2011**, 75(2), 361-422.
- 493 40. Müller, A. L.; Kjeldsen, K. U.; Rattei, T.; Pester, M.; Loy, A., Phylogenetic and environmental
494 diversity of DsrAB-type dissimilatory (bi)sulfite reductases. *Isme j* **2015**, 9(5), 1152-65.
- 495 41. Chen, J.; Yoshinaga, M.; Rosen, B. P., The antibiotic action of methylarsenite is an emergent
496 property of microbial communities. *Molecular microbiology* **2019**, 111(2), 487-494.
- 497 42. Achour, A. R.; Bauda, P.; Billard, P., Diversity of arsenite transporter genes from arsenic-resistant

- 498 soil bacteria. *Research in microbiology* **2007**, 158(2), 128-37.
- 499 43. Ruff, S. E.; Biddle, J. F.; Teske, A. P.; Knittel, K.; Boetius, A.; Ramette, A., Global dispersion and
500 local diversification of the methane seep microbiome. *Proceedings of the National Academy of*
501 *Sciences* **2015**, 112(13), 4015.
- 502 44. Inagaki, F.; Nunoura, T.; Nakagawa, S.; Teske, A.; Lever, M.; Lauer, A.; Suzuki, M.; Takai, K.;
503 Delwiche, M.; Colwell, F. S.; Nealson, K. H.; Horikoshi, K.; D'Hondt, S.; Jørgensen, B. B.,
504 Biogeographical distribution and diversity of microbes in methane hydrate-bearing deep marine
505 sediments on the Pacific Ocean Margin. *Proceedings of the National Academy of Sciences of the United*
506 *States of America* **2006**, 103(8), 2815.
- 507 45. Cai, L.; Liu, G.; Rensing, C.; Wang, G., Genes involved in arsenic transformation and resistance
508 associated with different levels of arsenic-contaminated soils. *BMC Microbiology* **2009**, 9(1), 4.
- 509 46. Silver, S.; Phung Le, T., Genes and Enzymes Involved in Bacterial Oxidation and Reduction of
510 Inorganic Arsenic. *Applied and Environmental Microbiology* **2005**, 71(2), 599-608.
- 511 47. Oremland, R. S.; Saltikov, C. W.; Stolz, J. F.; Hollibaugh, J. T., Autotrophic microbial
512 arsenotrophy in arsenic-rich soda lakes. *FEMS Microbiology Letters* **2017**, 364(15), fnx146.
- 513 48. van Lis, R.; Nitschke, W.; Duval, S.; Schoepp-Cothenet, B., Arsenics as bioenergetic substrates.
514 *Biochimica et biophysica acta* **2013**, 1827(2), 176-88.
- 515 49. Zhang, J.; Zhou, W.; Liu, B.; He, J.; Shen, Q.; Zhao, F. J., Anaerobic arsenite oxidation by an
516 autotrophic arsenite-oxidizing bacterium from an arsenic-contaminated paddy soil. *Environ Sci Technol*
517 **2015**, 49(10), 5956-64.
- 518 50. Rhine, E. D.; Phelps, C. D.; Young, L. Y., Anaerobic arsenite oxidation by novel denitrifying
519 isolates. *Environ Microbiol* **2006**, 8(5), 899-908.
- 520 51. Zhang, C.; Meckenstock, R. U.; Weng, S.; Wei, G.; Hubert, C. R. J.; Wang, J.-H.; Dong, X.,
521 Marine sediments harbor diverse archaea and bacteria with the potential for anaerobic hydrocarbon
522 degradation via fumarate addition. *FEMS Microbiology Ecology* **2021**, 97(5), fiab045.
- 523 52. Shi, L.-D.; Guo, T.; Lv, P.-L.; Niu, Z.-F.; Zhou, Y.-J.; Tang, X.-J.; Zheng, P.; Zhu, L.-Z.; Zhu,
524 Y.-G.; Kappler, A.; Zhao, H.-P., Coupled anaerobic methane oxidation and reductive arsenic
525 mobilization in wetland soils. *Nature Geoscience* **2020**, 13(12), 799-805.
- 526 53. Li, Y.; Guo, L.; Häggblom, M. M.; Yang, R.; Li, M.; Sun, X.; Chen, Z.; Li, F.; Su, X.; Yan, G.;
527 Xiao, E.; Zhang, H.; Sun, W., *Serratia* spp. Are Responsible for Nitrogen Fixation Fueled by As(III)
528 Oxidation, a Novel Biogeochemical Process Identified in Mine Tailings. *Environ Sci Technol* **2022**,
529 56(3), 2033-2043.
- 530 54. Li, Y.; Guo, L.; Yang, R.; Yang, Z.; Zhang, H.; Li, Q.; Cao, Z.; Zhang, X.; Gao, P.; Gao, W.; Yan,
531 G.; Huang, D.; Sun, W., *Thiobacillus* spp. and *Anaeromyxobacter* spp. mediate arsenite
532 oxidation-dependent biological nitrogen fixation in two contrasting types of arsenic-contaminated soils.
533 *Journal of hazardous materials* **2022**, 443(Pt A), 130220.
- 534 55. Zhang, C.; Fang, Y.-X.; Yin, X.; Lai, H.; Kuang, Z.; Zhang, T.; Xu, X.-P.; Wegener, G.; Wang,
535 J.-H.; Dong, X., The majority of microorganisms in gas hydrate-bearing subsurface sediments ferment
536 macromolecules. *bioRxiv* **2022**, 2022.05.19.492412.
- 537 56. Uritskiy, G. V.; DiRuggiero, J.; Taylor, J., MetaWRAP—a flexible pipeline for genome-resolved
538 metagenomic data analysis. *Microbiome* **2018**, 6(1), 158.
- 539 57. Li, D.; Liu, C.-M.; Luo, R.; Sadakane, K.; Lam, T.-W., MEGAHIT: an ultra-fast single-node

- 540 solution for large and complex metagenomics assembly via succinct de Bruijn graph. *Bioinformatics*
541 **2015**, 31(10), 1674-1676.
- 542 58. Nurk, S.; Meleshko, D.; Korobeynikov, A.; Pevzner, P. A., metaSPAdes: a new versatile
543 metagenomic assembler. *Genome Res* **2017**, 27(5), 824-834.
- 544 59. Nissen, J. N.; Johansen, J.; Allesøe, R. L.; Sønderby, C. K.; Armenteros, J. J. A.; Grønbech, C. H.;
545 Jensen, L. J.; Nielsen, H. B.; Petersen, T. N.; Winther, O.; Rasmussen, S., Improved metagenome
546 binning and assembly using deep variational autoencoders. *Nature Biotechnology* **2021**, 39(5),
547 555-560.
- 548 60. Parks, D. H.; Imelfort, M.; Skennerton, C. T.; Hugenholtz, P.; Tyson, G. W., CheckM: assessing
549 the quality of microbial genomes recovered from isolates, single cells, and metagenomes. *Genome Res*
550 **2015**, 25(7), 1043-1055.
- 551 61. Olm, M. R.; Brown, C. T.; Brooks, B.; Banfield, J. F., dRep: a tool for fast and accurate genomic
552 comparisons that enables improved genome recovery from metagenomes through de-replication. *The*
553 *Isme Journal* **2017**, 11(2864).
- 554 62. Kopylova, E.; Noé, L.; Touzet, H., SortMeRNA: fast and accurate filtering of ribosomal RNAs in
555 metatranscriptomic data. *Bioinformatics* **2012**, 28(24), 3211-3217.
- 556 63. Zhou, Z.; Tran, P.; Liu, Y.; Kieft, K.; Anantharaman, K., METABOLIC: a scalable
557 high-throughput metabolic and biogeochemical functional trait profiler based on microbial genomes.
558 *bioRxiv* **2019**, 761643.
- 559 64. Steinegger, M.; Söding, J., Clustering huge protein sequence sets in linear time. *Nature*
560 *Communications* **2018**, 9(1), 2542.
- 561 65. Delgado, L. F.; Andersson, A. F., Evaluating metagenomic assembly approaches for
562 biome-specific gene catalogues. *Microbiome* **2022**, 10(1), 72.
- 563 66. Keren, R.; Méheust, R.; Santini, J. M.; Thomas, A.; West-Roberts, J.; Banfield, J. F.;
564 Alvarez-Cohen, L., Global genomic analysis of microbial biotransformation of arsenic highlights the
565 importance of arsenic methylation in environmental and human microbiomes. *Comput Struct*
566 *Biotechnol J* **2022**, 20(559-572).
- 567 67. Lavy, A.; Matheus Carnevali, P. B.; Keren, R.; Bill, M.; Wan, J.; Tokunaga, T. K.; Williams, K. H.;
568 Hubbard, S. S.; Banfield, J. F., Taxonomically and metabolically distinct microbial communities with
569 depth and across a hillslope to riparian zone transect. *bioRxiv* **2020**, 768572.
- 570 68. Johnson, L. S.; Eddy, S. R.; Portugaly, E., Hidden Markov model speed heuristic and iterative
571 HMM search procedure. *BMC bioinformatics* **2010**, 11(431).
- 572 69. Chaumeil, P.-A.; Mussig, A.; Philip, H.; Parks, D., GTDB-Tk: a toolkit to classify genomes with
573 the Genome Taxonomy Database. *Bioinformatics* **2019**, 36(6), 1925-1927.
- 574 70. Shaffer, M.; Borton, M. A.; McGivern, B. B.; Zayed, A. A.; La Rosa, Sabina L.; Solden, L. M.;
575 Liu, P.; Narrowe, A. B.; Rodríguez-Ramos, J.; Bolduc, B.; Gazitúa, M. C.; Daly, R. A.; Smith, G. J.;
576 Vik, D. R.; Pope, P. B.; Sullivan, M. B.; Roux, S.; Wrighton, Kelly C., DRAM for distilling microbial
577 metabolism to automate the curation of microbiome function. *Nucleic Acids Res* **2020**, 48(16),
578 8883-8900.
- 579 71. Patro, R.; Duggal, G.; Love, M. I.; Irizarry, R. A.; Kingsford, C., Salmon provides fast and
580 bias-aware quantification of transcript expression. *Nature Methods* **2017**, 14(4), 417-419.
- 581 72. Katoh, K.; Standley, D. M., A simple method to control over-alignment in the MAFFT multiple

- 582 sequence alignment program. *Bioinformatics* **2016**, 32(13), 1933-42.
- 583 73. Capella-Gutiérrez, S.; Silla-Martínez, J. M.; Gabaldón, T., trimAl: a tool for automated alignment
584 trimming in large-scale phylogenetic analyses. *Bioinformatics* **2009**, 25(15), 1972-1973.
- 585 74. Nguyen, L. T.; Schmidt, H. A.; von Haeseler, A.; Minh, B. Q., IQ-TREE: a fast and effective
586 stochastic algorithm for estimating maximum-likelihood phylogenies. *Mol Biol Evol* **2015**, 32(1),
587 268-74.
- 588 75. Letunic, I.; Bork, P., Interactive tree of life (iTOL) v3: an online tool for the display and
589 annotation of phylogenetic and other trees. *Nucleic Acids Res* **2016**, 44(W1), W242-W245.
- 590

591 **ACKNOWLEDGMENTS**

592 This study was supported by the Scientific Research Foundation of Third Institute of
593 Oceanography, MNR (No. 2022025), the National Science Foundation of China (No.
594 41906076), the Science and Technology Projects in Guangzhou (No. 202102020970),
595 the Guangdong Basic and Applied Basic Research Foundation (No. 2019B030302004,
596 20201910240000691) and the Marine Geological Survey Program of China Geological
597 Survey (DD20221706).

598 **AUTHOR CONTRIBUTIONS**

599 XD designed this study with input from JL. CZ and XL analyzed omic data. XD, CZ,
600 XL, LDS and ZS interpreted data. JL and XX contributed to data collection. XD and CZ
601 drafted the paper, with input from all other authors.

602 **COMPETING INTERESTS**

603 The authors declare no competing interests.

604 **Figures Legends**

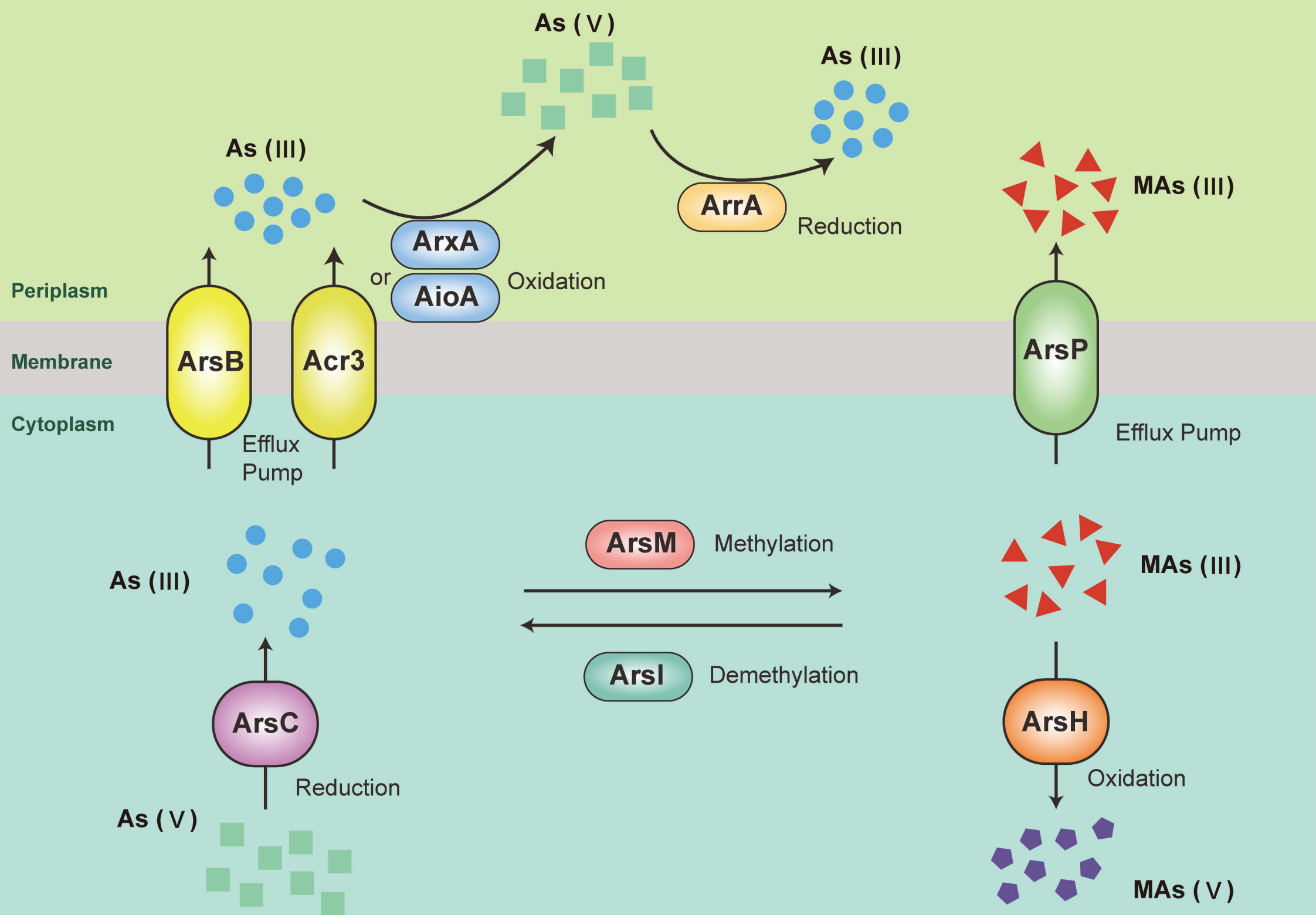
605 **Figure 1. Diagram of the microbial transformations of As.** As(III), arsenite; As(V),
606 arsenate; MMAs(III), trivalent methylarsenite; MMAs(V), pentavalentmethylarsenate.
607 As(III) efflux permease: ArsB/Acr3; cytoplasmic As(V) reductase: ArsC; respiratory
608 As(V) reductase: ArrA; As(III) oxidase: AioA/ArxA; As(III) S-adenosylmethionine
609 (SAM) methyltransferase: ArsM; non-heme iron-dependent dioxygenase: ArsI;
610 MAs(III) efflux permease: ArsP; MAs(III) oxidase: ArsH.

611 **Figure 2. The global distribution of potential genes involved in As cycling at cold**
612 **seeps.** (a) The abundances of As cycling genes across the 87 cold seep metagenomes.
613 The abundance of each gene was normalized by the gene length and sequencing depth
614 and represented as GPM (genes per million) value. (b) The partial least squares
615 discrimination analysis (PLS-DA) plots based on the abundances of As-cycling genes.
616 Similarity values among the samples of different sediment depths and types of cold
617 seep were examined using a 999-permutation PERMANOVA test. Source data is
618 available in **Table S2**.

619 **Figure 3. The community structures of microbiome involved in As cycling at cold**
620 **seeps.** The relative abundance of each MAG was estimated using CoverM. The
621 compositions of microbiome involved in As cycling across different types of cold
622 seep were clustered based the Bray-Curtis distance. Detailed statistics for As-related
623 microbiome are provided in **Table S4**.

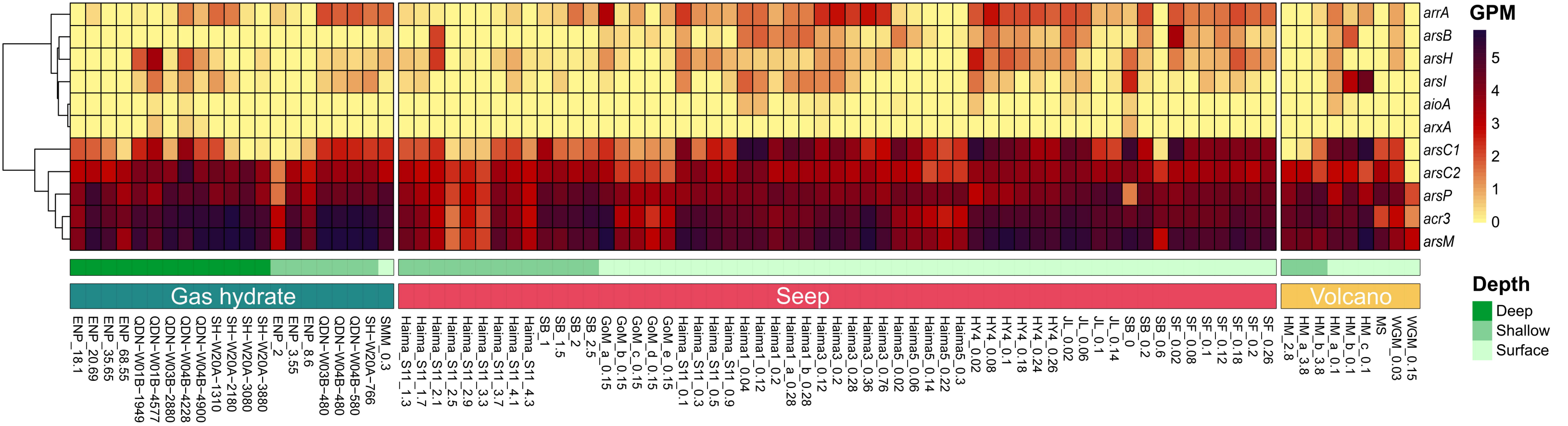
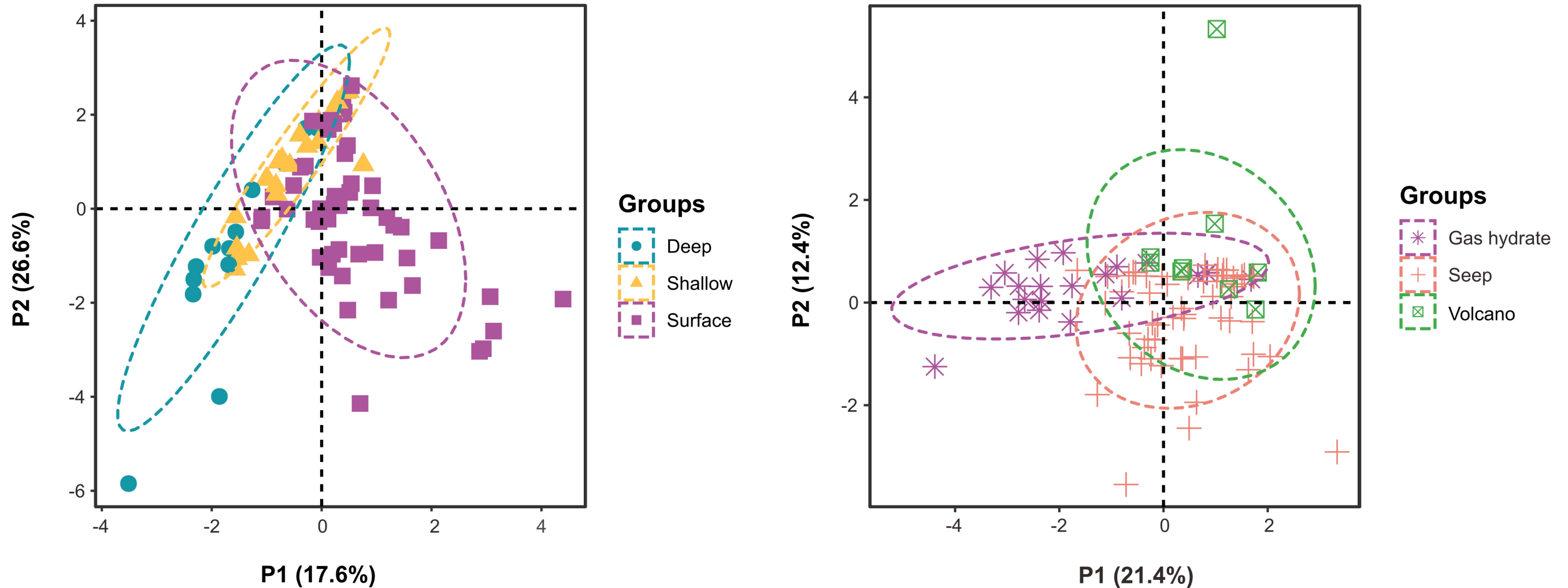
624 **Figure 4. Phylogenetic distribution of As-cycling genes.** Left bar plot showing the
625 total number of genomes encoded in each phylogenetic cluster assigned by GTDB-Tk
626 based on GTDB r207 release. Right bubble plot showing the number of As-cycling
627 genes encoded within each phylogenetic cluster. Detailed information on phylogenetic
628 diversity of As-cycling genes is provided in **Table S5**.

629 **Figure 5. The metabolic potential of the arsenotrophic gene-carrying MAGs.** (a)
630 A maximum-likelihood tree of the DMSO reductase family, with protein sequences
631 identified as associated with arsenotrophic enzymes in this study. Bootstrap values are
632 generated from 1000 replicates. Bootstrap values ≥ 70 are shown. Scale bar indicates
633 amino acid substitutions per site (b) The genomic context of the *aiiA*, *arxA* and *arrA*
634 clusters in MAGs containing arsenotrophic genes. (c) Heatmap showing the predicted
635 metabolism in potential As-respiring microbes. Detailed annotation is presented in
636 **Table S6.** The completeness of each pathway was calculated using the DRAM Distill
637 function.



a

bioRxiv preprint doi: <https://doi.org/10.1101/2022.11.20.517286>; this version posted November 21, 2022. The copyright holder for this preprint (which was not certified by peer review) is the author/funder. All rights reserved. No reuse allowed without permission.

**b**

Tree

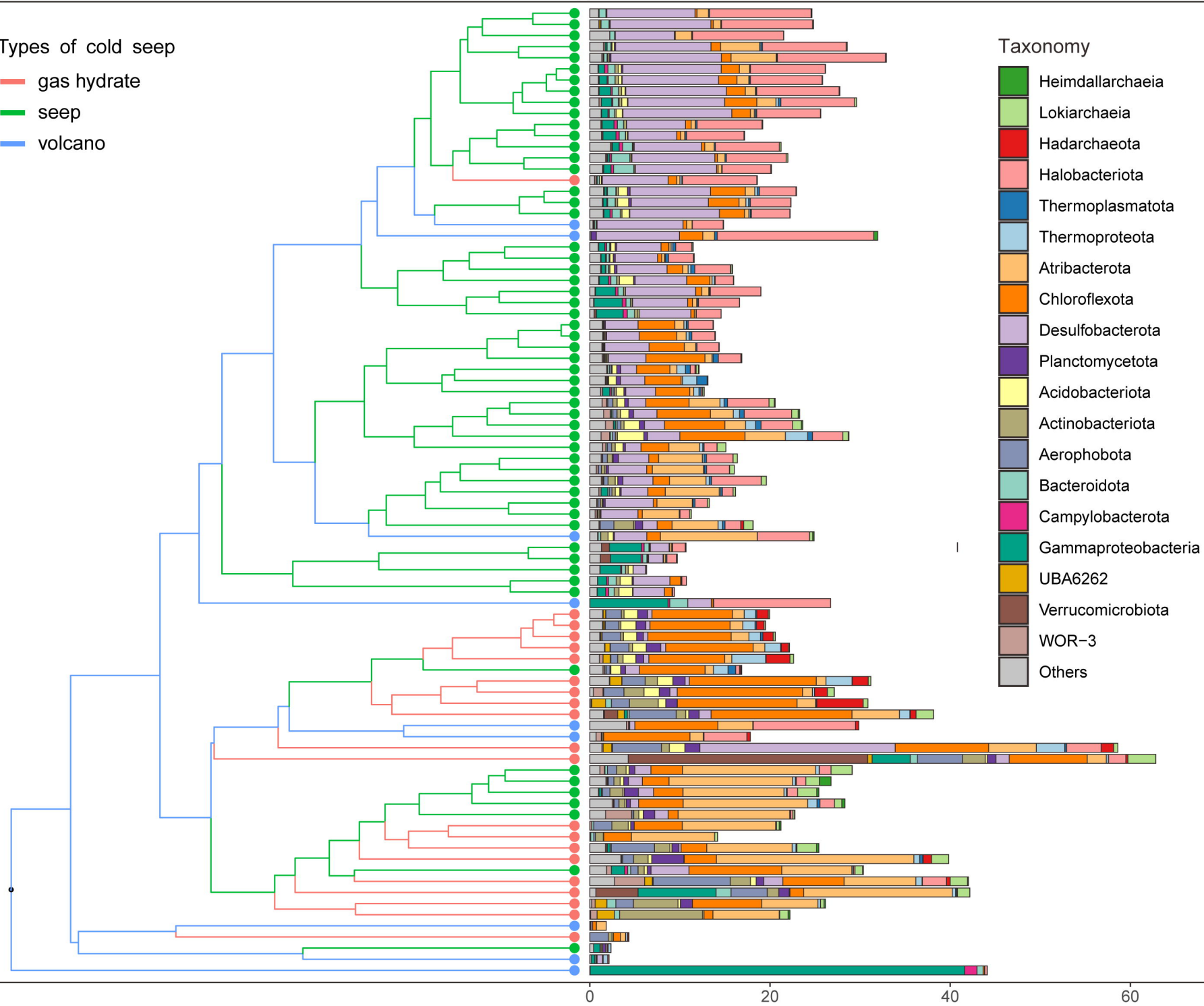
Relative abundance (%)

Types of cold seep

- gas hydrate
- seep
- volcano

Taxonomy

- Heimdallarchaeia
- Lokiarchaeia
- Hadarchaeota
- Halobacteriota
- Thermoplasmatota
- Thermoproteota
- Atribacterota
- Chloroflexota
- Desulfobacterota
- Planctomycetota
- Acidobacteriota
- Actinobacteriota
- Aerophobota
- Bacteroidota
- Campylobacterota
- Gammaproteobacteria
- UBA6262
- Verrucomicrobiota
- WOR-3
- Others



0

20

40

60

